Synthesis of galacto-oligosaccharides derived from lactulose by wild-type and mutant β-galactosidase enzymes from Bacillus circulans ATCC 31382

Yin, Huifang; Dijkhuizen, Lubbert; van Leeuwen, Sander

Published in:
Carbohydrate Research

DOI:
10.1016/j.carres.2018.06.009

Carbohydrate Research 465 (2018) 58–65

Contents lists available at ScienceDirect

Carbohydrate Research

journal homepage: www.elsevier.com/locate/carres

Synthesis of galacto-oligosaccharides derived from lactulose by wild-type and mutant β-galactosidase enzymes from *Bacillus circulans* ATCC 31382

Huifang Yin, Lubbert Dijkhuizen[1], Sander S. van Leeuwen[*,2]

Microbial Physiology, Groningen Biomolecular Sciences and Biotechnology Institute (GBB), University of Groningen, Nijenborgh 7, 9747 AG, Groningen, the Netherlands

ARTICLE INFO

Keywords:
Galactooligosaccharides
Lactulose
Structural characterization
Bacillus circulans β-galactosidase
NMR spectroscopy

ABSTRACT

Oligosaccharides derived from lactulose (β-D-Gal*p*-(1 → 4)-D-Fru) are drawing more and more attention nowadays because of their strong resistance to gut digestion, and the interest to discover novel prebiotics. Compared to galactooligosaccharides, currently known structures of lactulose oligosaccharides are very limited. In this study, the wild-type β-galactosidase BgaD-D of *Bacillus circulans* ATCC 31382, as well as the derived mutant R484H, were used to synthesize oligosaccharides from lactulose. In total, 9 oligosaccharide structures were identified by MALDI-TOF-MS and NMR spectroscopy analysis. Trisaccharide β-D-Gal*p*-(1 → 4)-β-D-Gal*p*-(1 → 4)-D-Fru was the major structure produced by the wild-type enzyme, while the R484H mutant showed a preference for synthesis of β-D-Gal*p*-(1 → 3)-β-D-Gal*p*-(1 → 4)-D-Fru. Our study greatly enriched the structural information about oligosaccharides derived from lactulose.

1. Introduction

Lactulose is a synthetic disaccharide (β-D-Gal*p*-(1 → 4)-D-Fru) that is usually produced by the isomerization of lactose using chemical catalysis [1–3], or enzymatic synthesis by various enzymes [4,5]. It is widely used in the pharmaceutical and food industry because of its healthy effect on humans, e.g. for the treatment of hepatic encephalopathy and constipation [6,7]. Lactulose is also known as a prebiotic which can stimulate the growth of Bifidobacteria and Lactobacilli, and modulate the microbial community composition and diversity in the gut [8–11]. Lactulose is mainly consumed by bacteria in the proximal colon, and may cause abdominal distension, intestinal gas production, and flatulence [7,12,13]. With the growing interest in new carbohydrate prebiotics with improved or complementary properties, galactooligosaccharides derived from lactulose (LGOS), containing one fructose residue, have been enzymatically synthesized and receive more and more attention [14–17].

It is well known that the resistance of oligosaccharides towards microbial degradation depends on the glycosidic linkages present, the monosaccharide composition, and the degree of polymerization (DP) [18–22]. Rapidly fermented carbohydrates mainly show bifidogenic effects in the caecum and proximal colon, while the more resistant oligosaccharides are able to reach the distal colon and influence the microbial composition there [23]. An *in vivo* study in rats showed that the disaccharide fraction of LGOS (β-galactobioses and galactosylfructoses) produced by *Aspergillus oryzae* was fully resistant to the digestion in the small intestine and completely fermented in the large intestine [24]. The trisaccharide fraction of LGOS was much more resistant to gut digestion (digestibility rates 12.5 ± 2.6%) than the trisaccharides from lactose derived galactooligosaccharides (GOS) (digestibility rates 52.9 ± 2.7%), and therefore these LGOS can reach the large intestine as carbon source for the intestinal microbiota [24].

LGOS and GOS synthesized by the *Aspergillus aculeatus* (Pectinex Ultra SP-L) and *Kluyveromyces lactis* (Lactozym 3000 L HP G) β-galactosidase enzymes from lactulose and lactose were both shown to have the ability to promote growth of Bifidobacteria using an *in vitro* fermentation system with human fecal cultures [23]. Another study showed that treatment with LGOS produced by the *A. oryzae* β-galactosidase changed the bacterial composition in the intestinal contents, resulting in increased numbers of Bifidobacteria and Lactobacilli [25]. This study also showed that LGOS generated a larger amount of short-chain fatty acids and showed a better anti-inflammatory effect than lactulose [25]. Short-chain fatty acids are the main fermentation products of these carbohydrates, and they exert health benefits to the host

Abbreviations: GOS, galactooligosaccharides; LGOS, galactooligosaccharides derived from lactulose; HPAEC-PAD, high-pH anion-exchange chromatography coupled with pulsed amperometric detection; NMR, nuclear magnetic resonance; MALDI-TOF-MS, Matrix Assisted Laser Desorption/Ionization-Time of Flight Mass Spectrometry; Gal, galactose; Fru, fructose; LGOS, oligosaccharides derived from lactulose

* Corresponding author.
E-mail address: s.s.van.leeuwen@umcg.nl (S.S. van Leeuwen).
[1] Current address: CarbExplore Research BV, Zernikepark 12, 9747 AG Groningen, The Netherlands.
[2] Current address: Department of Laboratory Medicine, University Medical Center Groningen, University of Groningen, 9713 GZ Groningen, The Netherlands.

https://doi.org/10.1016/j.carres.2018.06.009
Received 6 March 2018; Received in revised form 5 June 2018; Accepted 16 June 2018
Available online 19 June 2018
0008-6215/

[26,27]. LGOS produced by *A. oryzae* β-galactosidase also selectively increased the numbers of *Bifidobacterium animalis* in the caecum and colon of rats [28], greatly reduced intestinal pathogen adhesion [29], and enhanced iron absorption in the intestinal tract of rats [30].

New lactulose derived oligosaccharides may be used as functional food ingredients to improve gut health. Despite the extensive characterization and increasing studies of LGOS, there are only a limited number of structures synthesized and identified compared to oligosaccharides derived from lactose (GOS) [31–33]. One study found two LGOS trisaccharides, 6′-galactosyl-lactulose (β-D-Gal*p* (1 → 6)-β-D-Gal*p*-(1 → 4)-D-Fru), and 1-galactosyl-lactulose (β-D-Gal*p*-(1 → 4)-[β-D-Gal*p*-(1 → 1)-]β-D-Fru), as products from the transgalactosylation of lactulose by β-galactosidase from *A. aculeatus* [34]. Another study by this group identified the same two trisaccharides by incubating lactulose with β-galactosidase from *K. lactis* [35]. Padilla et al. identified 6-galactobiose, 6′-galactosyl-lactulose, and 1-galactosyl-lactulose as products from incubations of the crude cell extracts of 15 *Kluyveromyces* strains with lactulose [36]. Two lactulose oligosaccharides, allolactulose (β-D-Gal*p*-(1 → 6)-D-Fru) and 6′-galactosyl-lactulose, were identified as products of the transgalactosylation by β-galactosidase from *A. oryzae* [37]. Oligosaccharides up to a degree of polymerization (DP) of 6 were also detected from the transgalactosylation of *A. oryzae* β-galactosidase [38]. Another trisaccharide, 4′-galactosyl-lactulose (β-D-Gal*p*-(1 → 4)-β-D-Gal*p*-(1 → 4)-D-Fru), was formed when incubating cheese whey permeate with a commercial β-galactosidase from *Bacillus circulans* (Biocon) [16].

The *B. circulans* β-galactosidase is very effective in synthesizing GOS from lactose, producing a high-yield mixture with a broad structural spectrum [31,32]. In this study, we report the synthesis of LGOS from lactulose using the wild-type β-galactosidase BgaD-D enzyme from *B. circulans* [39,40] and a derived mutant (R484H) enzyme that has been described previously and showed a different structural composition of GOS from lactose [41], and the separation and identification of the products and their structures. In total 6 novel structures were identified.

2. Results and discussion

2.1. Optimization of LGOS yield

The LGOS yield was evaluated with different enzyme amounts, substrate concentrations, temperatures, and incubation times (Fig. 1). For the wild-type enzyme, the LGOS yield increased gradually when the enzyme units increased from 5 U/g lactulose to 15 U/g lactulose (Fig. 1A). When the enzyme amount was increased from 5 U/g to 10 U/g substrate, the LGOS yield of the R484H mutant enzyme remained similar. However, the LGOS yield of R484H enzyme increased greatly when the enzyme amount was 15 U/g (Fig. 1A). The influence of the substrate concentration on the LGOS yield was investigated at three lactulose concentrations: 40% (w/w), 50% (w/w), and 60% (w/w). For both wild-type and R484H enzymes, the LGOS yield increased when the substrate concentration increased, and both of them had the highest yield at 60% (w/w) lactulose concentration (Fig. 1B). The influence of temperatures on the LGOS yield was studied at 40 °C, 50 °C, and 60 °C. Both the wild-type BgaD-D and R484H enzymes had low LGOS yield at low temperatures. When the temperature increased, the LGOS yield also increased, and the highest yield was observed at 60 °C (Fig. 1C). Finally, the incubation durations were investigated for both enzymes at 8 h, 16 h, and 24 h reaction time. The wild-type enzyme had the highest LGOS yield at 8 h incubation. The R484H mutant had the highest LGOS yield at 16 h incubation (Fig. 1D).

In summary, when the enzyme units, substrate concentrations, and temperatures increased, the LGOS yield also increased. The incubation durations were not similarly correlated with the LGOS yield. The optimal condition for the wild-type enzyme was 60% (w/w) lactulose with 15 U/g enzyme activity at 60 °C incubated for 8 h, resulting in a yield of 202.9 ± 2.3 g/L (i.e. a conversion of lactulose into LGOS of 25.7%). The optimal condition for the R484H enzyme was the same as for WT, except for a longer incubation time of 16 h, with a yield of 197.7 ± 5.4 g/L (i.e. a conversion of lactulose into LGOS of 25.0%). It is reported that β-galactosidase from *A. oryzae* had a LGOS yield of 50% (w/v) at the optimal incubation conditions [37], while β-galactosidase from *Kluyveromyces marxianus* yielded 45 g LGOS from 100 g lactulose at its optimal reaction conditions [36]. Under the optimal incubation conditions found here, the yield of both the wild-type and R484H mutant enzymes therefore were clearly lower than the values reported for these other enzymes.

2.2. Characterization of LGOS

When incubated with lactose as only substrate, wild type BgaD-D prefers synthesizing GOS with (β1→4)-linkages, while the R484H mutant enzyme synthesizes GOS with (β1→3) and (β1→4)-linkages in comparable levels [41]. The LGOS mixtures produced by the wild-type BgaD-D and R484H mutant enzymes (10 U/mL, 50% (w/w) lactulose, 50 °C, 20 h incubation) were analyzed by Matrix-assisted Laser Desorption Ionization – Time of Flight Mass spectrometry (MALDI-TOF-MS) (Fig. 2). Both enzymes produced relatively short LGOS from lactulose, with mainly DP2 (*m/z* 364.8 Da) and DP3 (*m/z* 526.8 Da), a minor amount of DP4 (*m/z* 689.0 Da) and only trace amounts of DP5 (*m/z* 851.1 Da) (Fig. 2). When incubated with lactose both enzymes are capable of synthesizing GOS of much higher DP [41,42]. Analysis by High-pH Anion Exchange Chromatography with Pulsed Amperometric Detection (HPAEC-PAD) rendered profiles of the LGOS synthesized by WT and R484H mutant enzymes showed that a large quantity of lactulose remained (Fig. 3).

A pre-fractionation on BioGel P2 rendered sub-pools containing DP3 – DP5 structures (not shown). The two relevant sub-pools were fractionated further by preparative HPAEC-PAD on a CarboPac PA-1 column (9 × 250 mm; Dionex). Isolated fractions were analyzed by NMR spectroscopy and MALDI-TOF-MS. MALDI-TOF-MS analysis of the isolated fractions showed peaks at *m/z* 527.1 for fractions **1–5** fitting the sodium adduct of trisaccharide structures. Fractions **6** and **7** showed a peak at *m/z* 689.2 Da fitting the sodium adduct of tetrasaccharide structures. Reinjection on an analytical HPAEC-PAD column confirmed the elution positions of the isolated fractions (Fig. 3).

2.2.1. Fraction *1*

The 1D ^{1}H NMR spectrum of trisaccharide **1** (Fig. S1) showed β-anomeric signals at δ 4.638 (**B**^{p} H-1; $J_{1,2}$ 8.0 Hz) and δ 4.510 (**C**^{p} H-1; $J_{1,2}$ 8.1 Hz). The signal at δ 4.418 ($J_{3,4}$ 2.8 Hz) typically fits with the H-5 signal of a fructopyranose residue. It is, however, shifted significantly downfield, compared with lactulose [43] (δH-5 4.199). The characteristic peaks for the furanose form δ H-3 4.29 and δ H-4 4.26 are absent in the 1D ^{1}H NMR spectrum. Starting from the β-anomeric signals for the Gal residues, and the fructose H-5 the ^{1}H chemical shifts of **B**^{p} and **C**^{p} could be determined up to H-4 and for **A**$_{p}$ from H-3 to H-6a,b from the COSY and TOCSY spectra (Table 1). The H-5 and H-6a,b signals for the Gal residues and the H-1a,b signals of **A**$_{p}$ were derived from the HSQC. The identity of **A**$_{p}$ H-1a and H-1b were confirmed by the observation that H-1a at δ 3.534 only correlated in COSY and TOCSY spectra with δ 3.783, which fits with H-1b.

The clear downfield shift of the **A**$_{p}$ H-5 and C-5 signals to δ 4.418 ($\Delta\delta$ + 0.22) and δ 74.2 ($\Delta\delta$ + 6.5) indicate a 5-substitution of the Fru residue [31–33,43]. This is further supported by the ROESY interresidual correlations between **C**^{p} H-1 and **A**$_{p}$ H-5 and between **C**^{p} H-1 and **A**$_{p}$ H-6a,b (Fig. S1). The linkage between residue **B** and O4 of fru residue **A** is further confirmed by ROESY correlations between **B**^{p} H-1 and **A**$_{p}$ H-4 and between **B**^{p} H-1 and **A**$_{p}$ H-5 (Fig. S1). The substitution at **A** O5 explains the absence of the peaks corresponding with the furanose form, since closure of the ring in furanose form requires a free OH-5. These data lead to the conclusion that trisaccharide **1** has a β-D-Gal*p*-(1 → 5)[β-D-Gal*p*-(1 → 4)]-D-Fru*p* structure; i.e. **C**1→5 [**B**1→4]**A** (Fig. 3).

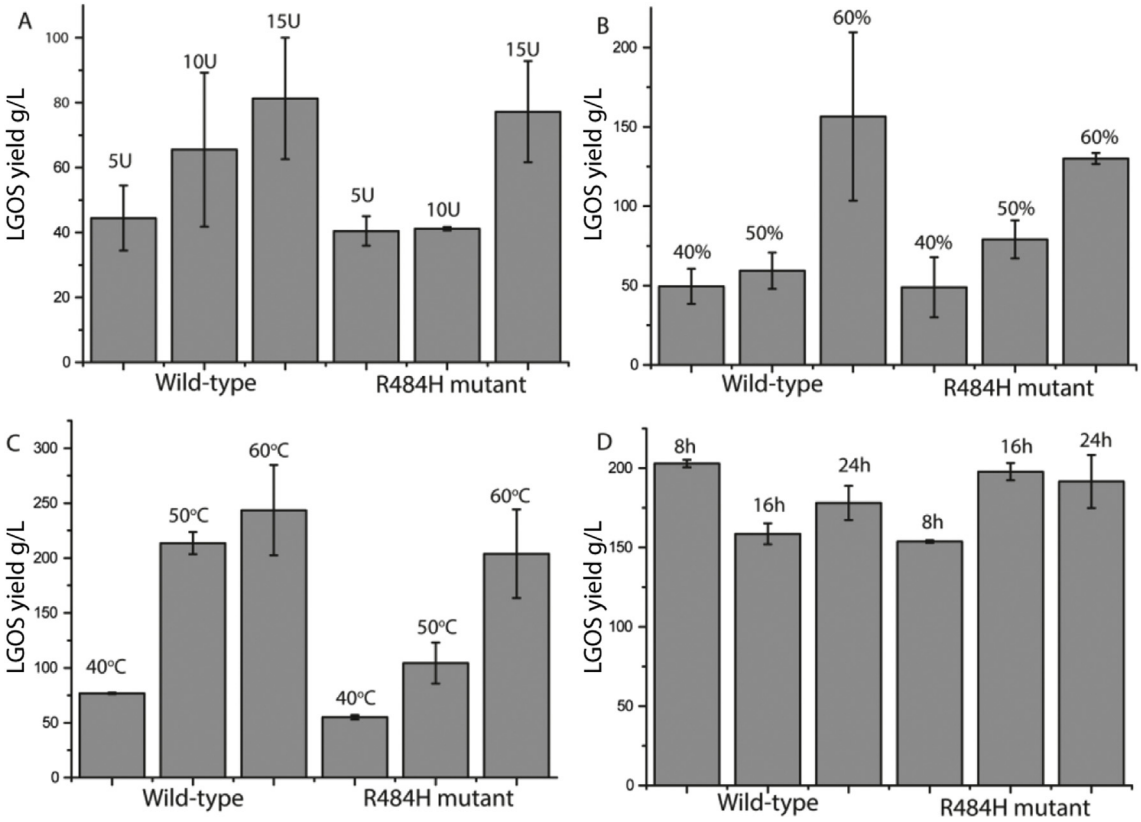

Fig. 1. Effect of (A) enzyme units, (B) lactulose concentrations, (C) temperatures, and (D) incubation times on LGOS yield of the wild-type and R484H mutant β-galactosidase enzymes. Data obtained from duplicate experiments. Incubation conditions: (A) 50% (w/w) lactulose solution, incubated at 50 °C for 8 h; (B) 15 U/g enzyme, incubated at 50 °C for 8 h; (C) 15 U/g enzyme, 60% (w/w) lactulose solution for 8 h; (D) 15 U/g enzyme, 60% (w/w) lactulose solution, 60 °C.

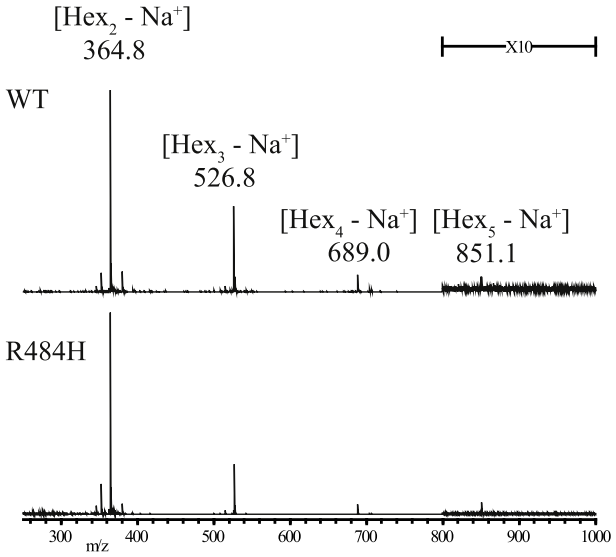

Fig. 2. MALDI-TOF-MS analysis of LGOS produced from lactulose by the wild-type BgaD-D and R484H mutant *B. circulans* ATCC 31382 enzymes. Hex: hexose unit.

2.2.2. Fraction 2

The 1D ^{1}H NMR spectrum of fraction **2** (Fig. S2) showed anomeric signals belonging to two separate trisaccharide compounds **2a** and **2b**. Anomeric signals at δ 4.472 (**B**^{f} H-1; $J_{1,2}$ 7.8 Hz) and δ 4.510 (**C**^{f} H-1; $J_{1,2}$ 8.0 Hz) are assigned to structure **2a** and anomeric signals δ 4.576 (**B**^{p} H-1; $J_{1,2}$ 7.8 Hz), δ 4.504 (**B**^{f} H-1; $J_{1,2}$ 7.7 Hz), and 4.517 (**C** H-1; $J_{1,2}$ 8.0 Hz) were assigned to structure **2b**. Using 2D NMR spectroscopy all ^{1}H and most ^{13}C chemical shifts could be assigned for both structures (Table 1). For structure **2a** residue **A**$_{f}$ showed an altered pattern. Particularly H-6a and H-6b (δ 4.17; 3.83) showed a very large downfield shift, compared with **A**$_{f}$ of lactulose. The C-6 chemical shift δ 72.0, indicated a 6-substitution of residue **A**$_{f}$. For structure **2a** no **A**$_{p}$ residue was observed, fitting with a 6-substitution. Further the position of H-4 and C-4 (δ^{1}H 4.33; δ^{13}C 75.4) fit with the 4-substitution of residue **A**$_{f}$. Residues **B** and **C** both show the chemical shift pattern of a terminal Gal residue [31–33]. The ROESY inter-residual correlations between **B** H-1 and **A** H-4 and between **C** H-1 and **A** H-6a,b support the substitution patterns. These data lead to a structure for **2a** of β-D-Gal*p*-(1 → 6)[β-D-Gal*p*-(1 → 4)]-D-Fru; i.e. **C**1→6 [**B**1→4]**A** for structure **2a** (Fig. 3).

For structure **2b** residue **A** showed a chemical shift pattern matching with that of lactulose, indicating a 4-substituted Fru residue. Residue **B** showed H-6a and H-6b shifted downfield, combined with a C-6 shifted downfield to δ 70.0, indicating a 6-substituted residue. Residue **C** showed a pattern fitting a terminal Gal residue [31–33]. The ROESY inter-residual correlations between **B** H-1 and **A** H-4, and between **C** H-1 and **B** H-6a,b further support these findings. All data result in a structure for **2b** of β-D-Gal*p*-(1 → 6)-β-D-Gal*p*-(1 → 4)-D-Fru; i.e. **C**1→6**B**1→4**A** (Fig. 3).

2.2.3. Fraction 3

The trisaccharide **F3** showed a 1D ^{1}H NMR spectrum (Fig. S3) with β-anomeric signals at δ 4.561 (**B**^{p} H-1; $J_{1,2}$ 7.9 Hz), δ 4.469 (**B**^{f} H-1; $J_{1,2}$ n. d), and δ 4.445 (**C** H-1; $J_{1,2}$ 8.0 Hz). From the 2D NMR spectra all ^{1}H chemical shifts and most ^{13}C chemical shifts could be assigned (Table 1). Both residues **B** and **C** show a chemical shift pattern fitting a terminal Gal residue. The splitting of the Gal anomeric signals based on the furanose and pyranose mutarotamers of the Fru residue suggests that both residues are linked to the Fru residue. The H-1a and H-1b signals of the Fru residue are shifted significantly, compared with Fru in

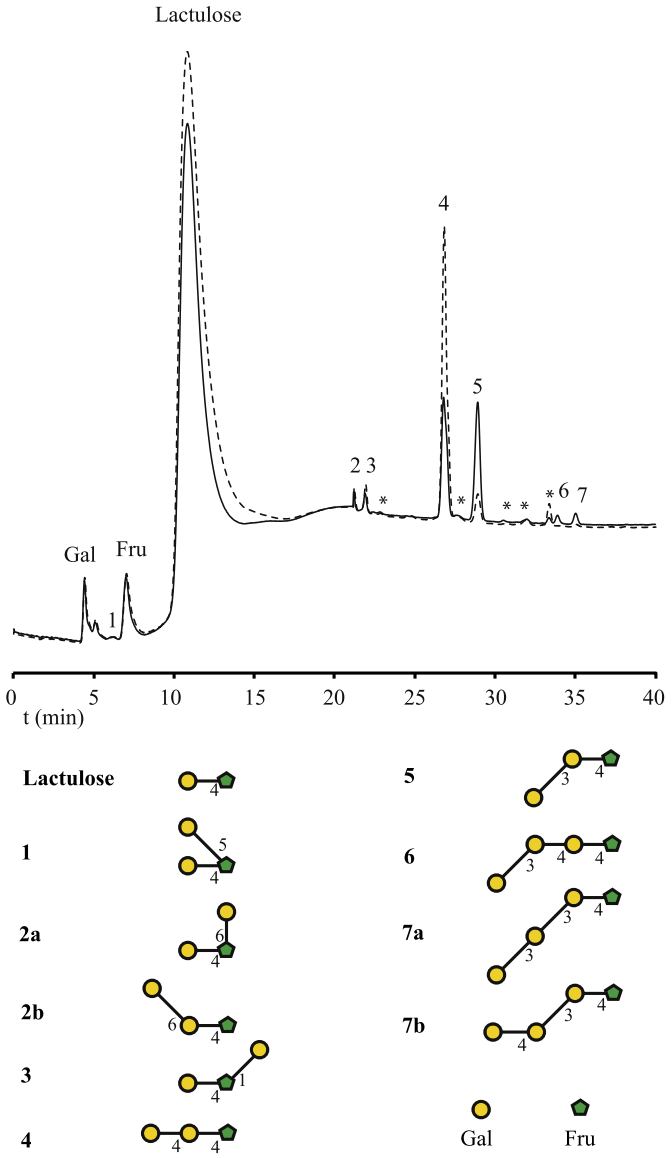

Fig. 3. HPAEC-PAD analysis of LGOS produced by the wild-type BgaD-D and R484H mutant enzymes (left), and the identified LGOS structures (right). Peaks marked with * were shown to be LGOS by distinctive peaks in the 1D ^{1}H NMR spectrum, but were of insufficient quantity to identify.

lactulose. Moreover, the HSQC spectrum showed C-1 of Fru shifted significantly downfield, indicating a 1-substitution of the Fru residue. The ROESY spectrum showed interresidual correlations between **B** H-1 and **A** H-4 and between **C** H-1 and **A** H-1a,b. These data result in the postulated structure for **3** of β-D-Gal*p*-(1 → 4)[β-D-Gal*p*-(1 → 1)]-D-Fru; i.e. **B**1→4 [**C**1→1]**A** (Fig. 3).

2.2.4. Fraction 4

The 1D ^{1}H NMR spectrum of trisaccharide **4** (Fig. S4) showed β-anomeric peaks at δ 4.610 (**C** H-1; $J_{1,2}$ 7.8 Hz), δ 4.593 (**B**^{p} H-1; $J_{1,2}$ 8.1 Hz) and δ 4.501 (**B**^{f} H-1; $J_{1,2}$ 8.1 Hz). From the 2D NMR spectra all ^{1}H and ^{13}C chemical shifts could be assigned (Table 1). The signals for the $\mathbf{A}_p$ and $\mathbf{A}_f$ matched closely with that observed for the Fru residue in lactulose, confirming no further substitution on this residue. Residue **B** showed a significant downfield shift in H-3 ($\Delta\delta$ +0.08) and H-4 ($\Delta\delta$ +0.29) compared with lactulose. The C-4 is also shifted downfield to δ 78.1, indicative of a 4-substituted residue **B** [31–33]. This observation is supported by the interresidual correlation between **C** H-1 and **B** H-4 observed in the 2D ROESY spectrum. These data result in a structure for **4** of β-D-Gal*p*-(1 → 4)-β-D-Gal*p*-(1 → 4)-D-Fru; i.e. **C**1→4**B**1→4**A** (Fig. 3).

2.2.5. Fraction 5

The 1D ^{1}H NMR spectrum of trisaccharide **5** (Fig. S5) showed β-anomeric peaks at δ 4.619 (**B**^{p} H-1; $J_{1,2}$ 7.7 Hz), δ 4.616 (**C** H-1; $J_{1,2}$ 7.6 Hz) and δ 4.526 (**B**^{f} H-1; $J_{1,2}$ 7.8 Hz). From the 2D NMR spectra all ^{1}H and ^{13}C chemical shifts could be assigned (Table 1). The signals for the $\mathbf{A}_p$ and $\mathbf{A}_f$ matched closely with that observed for the Fru residue in lactulose, confirming no further substitution on this residue. Residue **B** showed a significant downfield shift in H-3 ($\Delta\delta$ +0.17) and H-4 ($\Delta\delta$ +0.31). The C-3 is shifted downfield to δ 83.2, supporting a 3-substitution of residue **B** [31–33]. The O3 substitution at residue **B** is confirmed by the interresidual correlation between **C** H-1 and **B** H-3 observed in the 2D ROESY spectrum. These data result in a structure for **5** of β-D-Gal*p*-(1 → 3)-β-D-Gal*p*-(1 → 4)-D-Fru; i.e. **C**1→3**B**1→4**A** (Fig. 3).

2.2.6. Fraction 6

The 1D ^{1}H NMR spectrum of tetrasaccharide **6** (Fig. S6) showed β-anomeric signals at δ 4.666 (**C** H-1; $J_{1,2}$ 7.8 Hz), δ 4.617 (**D** H-1; $J_{1,2}$ 7.6 Hz), δ 4.591 (**B**^{p} H-1; $J_{1,2}$ 7.8 Hz), and δ 4.500 (**B**^{f} H-1; $J_{1,2}$ 7.7 Hz). Using 2D NMR spectroscopy all ^{1}H chemical shifts and part of the ^{13}C chemical shifts were assigned (Table 1). The chemical shift pattern of residue **A** matches that of lactulose fitting with a reducing Fru residue that is 4-substituted. Residue **B** has an H-1 signal that is shifted downfield compared with residue **B** in lactulose. Moreover, the H-3 and H-4 are shifted downfield, and also C-4 showed a downfield shift, fitting with a 4-substituted residue **B**. Residue **C** showed also a H-3 and H-4 that are shifted downfield, in this case H-3 is shifted further downfield than for residue **B**. Residue **C** has a C-3 that is shifted downfield, indicating a 3-substituted residue [31–33]. Residue **D** has a pattern of chemical shifts fitting a terminal Gal residue. The glycosidic linkages between the residues is further shown by interresidual ROESY correlations between **D** H-1 and **C** H-3, between **C** H-1 and **B** H-4 and between **B** H-1 and **A** H-4. These data result in a structure for **6** of β-D-Gal*p*-(1 → 3)-β-D-Gal*p*-(1 → 4)-β-D-Gal*p*-(1 → 4)-D-Fru; i.e. **D**1→3**C**1→4**B**1→4**A** for structure **6** (Fig. 3).

2.2.7. Fraction 7

Fraction **7** contains two major tetrasaccharide structures. The β-anomeric signals in the 1D ^{1}H NMR spectrum (Fig. S7) at δ 4.679 (**C** H-1; $J_{1,2}$ 7.9 Hz), δ 4.619 (**B**^{p} H-1; $J_{1,2}$ 7.8 Hz), δ 4.615 (**D** H-1; $J_{1,2}$ 7.9 Hz), and δ 4.523 (**B**^{f} H-1; $J_{1,2}$ 7.6 Hz) were assigned to structure **7a**. The signals at δ 4.658 (**C** H-1; $J_{1,2}$ 7.9 Hz), δ 4.619 (**B**^{p} H-1; $J_{1,2}$ 7.8 Hz), 4.600 (**D** H-1; $J_{1,2}$ 8.2 Hz), and δ 4.520 (**B**^{f} H-1; $J_{1,2}$ 8.1 Hz) were assigned to structure **7b**. Starting from the anomeric signals in the 2D NMR spectra all ^{1}H chemical shifts could be assigned for **7a** (Table 1) for the Gal residues. Starting from the **A** H-4 signals at δ 4.14 and δ 4.28 the ^{1}H chemical shifts of the Fru residue were assigned, except for the H-1a and H-1b signals, which were derived from the HSQC spectrum. From the 2D HSQC spectrum most ^{13}C assignments were possible. The chemical shift pattern observed for residues **C** and **B** fits with that of a 3-substituted β-D-Gal*p* residue. Residue **D** showed a pattern fitting a terminal residue. The chemical shifts for the Fru residue match that of the Fru residue in lactulose, indicating a 4-substituted residue. The connections between the residues are further supported by ROESY interresidual correlations between **D** H-1 and **C** H-3, between **C** H-1 and **B** H-3, and between **B** H-1 and **A** H-4. These data result in the structure for **7a** of β-D-Gal*p*-(1 → 3)-β-D-Gal*p*-(1 → 3)-β-D-Gal*p*-(1 → 4)-D-Fru; i.e. **D**1→3**C**1→3**B**1→4**A** (Fig. 3).

Also for structure **7b** all ^{1}H chemical shifts and most ^{13}C chemical shifts could be obtained from the 2D NMR spectra (Table 1). The Fru residue **A** showed chemical shifts corresponding with those observed in lactulose, indicating a 4-substituted Fru residue. Residues **B**^{p} and **B**^{f} showed patterns similar to resiue **B** in structures **5** and **7a**, indicating a

Table 1
Proton and carbon chemical shifts of structures **1–7**, determined by 1D and 2D NMR spectroscopy in reference to internal acetone (δ^1H 2.225; δ^{13}C 31.08).

	Lactulose		1		2a		2b		3	
	^{1}H	^{13}C	^{1}H	^{13}C	^{1}H	^{13}C	^{1}H	^{13}C	^{1}H	^{13}C
A_p^i 1a	3.71	64.8	3.534	64.4			3.71	65.0	3.96	72.6
A_p 1b	3.57	64.8	3.783	64.4			3.57	65.0	3.87	72.6
A_p 3	3.93	67.0	3.990	66.7			3.93	67.1	3.96	67.2
A_p 4	4.132	78.4	4.254	76.7			4.13	79.1	4.15	78.0
A_p 5	4.199	67.7	4.418	74.2			4.21	68.0	4.21	67.7
A_p 6a	4.019	63.9	3.949	61.2			4.02	64.1	4.06	63.9
A_p 6b	3.75	63.9	3.949	61.2			3.75	64.1	3.74	63.9
A_f 1a	3.60	63.4			3.60	63.5	3.60	63.5	3.98	72.4
A_f 1b	3.55	63.4			3.55	63.5	3.55	63.5	3.74	72.4
A_f 3	4.29	75.4			4.29	75.4	4.29	75.4	4.36	75.4
A_f 4	4.26	85.1			4.33	85.3	4.26	85.3	4.27	n.d.
A_f 5	4.03	80.9			4.29	79.6	4.03	n.d.	4.06	n.d.
A_f 6a	3.81	63.4			4.17	72.0	3.80	63.6	n.d.	n.d.
A_f 6b	3.71	63.4			3.83	72.0	3.69	63.6	n.d.	n.d.
B^p 1	4.557	101.6	4.638	n.d.			4.576	101.8	4.561	n.d.
B^p 2	3.60	71.5	3.60	71.6			3.63	71.6	3.60	71.7
B^p 3	3.68	73.5	3.68	73.5			3.69	73.8	3.68	73.4
B^p 4	3.92	69.5	3.925	69.5			3.97	69.7	3.92	69.6
B^p 5	3.71	76.3	3.71	76.2			3.92	75.4	3.71	76.1
B^p 6a	3.82	62.0	3.81	61.9			4.060	70.0	3.75	62.0
B^p 6b	3.75	62.0	3.76	61.9			3.94	70.0	3.80	62.0
B^f 1	4.464	103.8			4.472	103.4	4.504	103.4	4.469	n.d.
B^f 2	3.56	71.5			3.58	71.8	3.59	71.6	3.57	71.7
B^f 3	3.66	73.5			3.66	73.6	3.67	73.8	3.67	73.4
B^f 4	3.92	69.5			3.92	69.7	3.97	69.7	3.92	69.6
B^f 5	3.71	76.3			3.70	76.4	3.92	75.4	3.71	76.1
B^f 6a	3.82	62.0			3.80	62.1	4.060	70.0	3.75	62.0
B^f 6b	3.75	62.0			3.75	62.1	3.94	70.0	3.80	62.0
C 1			4.510	103.6	4.478	104.4	4.517	104.4	4.445	n.d.
C 2			3.58	71.6	3.59	71.8	3.55	71.6	3.57	71.7
C 3			3.66	73.5	3.66	73.6	3.66	73.8	3.66	73.4
C 4			3.925	69.5	3.92	69.7	3.92	69.7	3.92	69.6
C 5			3.71	76.2	3.70	76.4	3.70	76.4	3.71	76.1
C 6a			3.81	61.9	3.80	61.2	3.80	62.1	3.75	62.0
C 6b			3.76	61.9	3.75	61.2	3.75	62.1	3.80	62.0

	4		5		6		7a		7 b	
	^{1}H	^{13}C	^{1}H	^{13}C	^{1}H	^{13}C	^{1}H	^{13}C	^{1}H	^{13}C
A_p 1a	3.74	64.7	3.71	65.0	3.72	64.9	3.71	64.9	3.71	64.9
A_p 1 b	3.58	64.7	3.57	65.0	3.59	64.9	3.59	64.9	3.59	64.9
A_p 3	3.924	66.9	3.929	67.2	3.92	67.5	3.92	67.5	3.92	67.5
A_p 4	4.13	78.2	4.146	78.4	4.128	78.3	4.14	78.3	4.14	78.3
A_p 5	4.21	67.4	4.21	67.7	4.20	67.8	4.20	67.8	4.20	67.8
A_p 6a	4.02	63.9	4.019	64.0	4.02	64.2	4.017	64.2	4.017	64.2
A_p 6b	3.75	63.9	3.75	64.0	3.75	64.2	3.75	64.2	3.75	64.2
A_f 1a	3.58	63.3	3.600	63.6	3.60	63.8	3.60	63.8	3.60	63.8
A_f 1b	3.58	63.3	3.55	63.6	3.55	63.8	3.55	63.8	3.55	63.8
A_f 3	4.295	75.5	4.31	75.2	4.29	n.d.	4.28	75.6	4.28	75.6
A_f 4	4.273	85.0	4.288	85.2	4.26	n.d.	4.26	85.1	4.26	85.1
A_f 5	4.016	80.9	4.05	81.0	4.04	n.d.	4.04	81.0	4.04	81.0
A_f 6a	3.81	63.4	3.81	63.8	3.81	64.0	3.81	64.0	3.81	64.0
A_f 6b	3.69	63.4	3.71	63.8	3.72	64.0	3.72	64.0	3.72	64.0
B^p 1	4.593	101.8	4.619	101.6	4.591	101.3	4.619	n.d.	4.619	n.d.
B^p 2	3.69	71.9	3.77	71.1	3.69	71.9	3.77	71.8	3.77	71.8
B^p 3	3.79	73.7	3.85	83.2	3.79	73.9	3.84	74.0	3.84	83.3
B^p 4	4.198	78.1	4.206	69.6	4.21	78.6	4.20	78.5	4.20	69.2
B^p 5	3.76	76.1	3.70	76.2	3.75	75.5	3.71	76.0	3.73	75.7
B^p 6a	3.83	61.6	3.72	62.0	3.75	62.0	3.75	62.0	3.75	62.0
B^p 6b	3.77	61.6	3.80	62.0	3.80	62.0	3.80	62.0	3.80	62.0
B^f 1	4.501	103.6	4.526	103.6	4.500	103.5	4.523	n.d.	4.520	n.d.
B^f 2	3.65	71.9	3.73	71.1	3.65	72.2	3.73	72.3	3.73	71.8
B^f 3	3.78	73.7	3.85	83.2	3.78	73.9	3.84	83.3	3.84	83.3
B^f 4	4.187	78.1	4.194	69.6	4.19	73.8	4.20	69.2	4.16	69.2
B^f 5	3.76	76.1	3.71	76.2	3.75	75.5	3.71	76.0	3.73	75.7
B^f 6a	3.83	61.6	3.72	62.0	3.75	62.0	3.75	62.0	3.75	62.0
B^f 6b	3.77	61.6	3.80	62.0	3.80	62.0	3.80	62.0	3.80	62.0

(*continued on next page*)

Table 1 (*continued*)

	4		5		6		7a		7 b	
	^{1}H	^{13}C	^{1}H	^{13}C	^{1}H	^{13}C	^{1}H	^{13}C	^{1}H	^{13}C
C 1	4.610	105.0	4.616	105.5	4.666	105.3	4.679	n.d.	4.658	n.d.
C 2	3.58	71.9	3.61	72.1	3.74	71.6	3.78	71.8	3.68	71.8
C 3	3.67	73.7	3.67	73.6	3.84	83.4	3.84	83.3	3.74	73.6
C 4	3.904	69.7	3.917	69.7	4.18	69.3	4.20	69.2	4.18	78.1
C 5	3.71	76.1	3.71	76.2	3.70	75.9	3.71	76.0	3.71	76.0
C 6a	3.83	61.0	3.72	62.0	3.75	62.0	3.75	62.0	3.75	62.0
C 6b	3.77	61.0	3.80	62.0	3.80	62.0	3.80	62.0	3.80	62.0
D 1					4.617	105.6	4.615	n.d.	4.600	n.d.
D 2					3.61	72.2	3.60	72.3	3.58	72.3
D 3					3.68	73.7	3.66	73.6	3.66	73.6
D 4					3.92	69.6	3.92	69.6	3.90	69.6
D 5					3.71	75.9	3.71	76.0	3.71	76.0
D 6a					3.75	62.0	3.75	62.0	3.75	62.0
D 6b					3.80	62.0	3.80	62.0	3.80	62.0

[i] Residue label A_p signifies a Fru residue that is in pyranose form, whereas A_f indicates a Fru*f* residue. Residues B^p and B^f stand for Gal residue B that is linked to a Fru*p* or a Fru*f* residue, respectively.

3-substituted Gal residue. For residue **C** a pattern was observed fitting a 4-substituted residue and residue **D** had a pattern fitting a terminal β-D-Gal*p*-residue. The connections between the residues are further confirmed by interresidual correlations between **D** H-1 and **C** H-4, between **C** H-1 and **B** H-3 and between **B** H-1 and **A** H-4 signals. These data result in a structure for **7b** of β-D-Gal*p*-(1 → 4)-β-D-Gal*p*-(1 → 3)-β-D-Gal*p*-(1 → 4)-D-Fru; i.e. **D**1→4**C**1→3**B**1→4**A** (Fig. 3).

LGOS derived from the wild-type BgaD-D and R484H mutant enzymes both contained structures **1–5** (Fig. 3). Structures **6** and **7** were only found in the LGOS derived from the R484H mutant enzyme. Some minor peaks were visible as well but could not be identified (Fig. 3). The wild-type enzyme produced more structure **4** (β-D-Gal*p*-(1 → 4)-β-D-Gal*p*-(1 → 4)-D-Fru) than the R484H mutant enzyme, while the R484H mutant enzyme produced more structure **5** (β-D-Gal*p*-(1 → 3)-β-D-Gal*p*-(1 → 4)-D-Fru), and F7 (β-D-Gal*p*-(1 → 3)-β-D-Gal*p*-(1 → 3)-β-D-Gal*p*-(1 → 4)-D-Fru). This observed difference in preference fits with what was found for these two enzymes in the GOS products synthesized from lactose [41]. The relatively high level of structure **5** in the wild-type product, however, does not fit with the observation that only trace amounts of 3′-galactosyllactose was formed from lactose [41]. The study by Corzo-Martínez et al. identified structure **4** in the LGOS derived from the commercial *B. circulans* β-galactosidase enzyme (Biocon, Spain) [16]. Here, we identified 9 LGOS structures in total, including the structures found by Cardelle-Cobas et al. [44], namely **2b** (β-D-Gal*p*-(1 → 6)-β-D-Gal*p*-(1 → 4)-D-Fru) and **3** (β-D-Gal*p*-(1 → 4)-[β-D-Gal*p*-(1 → 1)]-D-Fru). However, allolactulose (β-D-Gal*p*-(1 → 6)-D-Fru) found in the LGOS produced by *A. oryzae* β-galactosidase by Cardelle-Cobas et al. [37], was not observed in our study. Compared with previous studies, we identified and characterized a total of 6 novel LGOS structures, i.e. **1**, **2a**, **5**, **6**, **7a**, and **7b** (Fig. 3).

3. Conclusions and perspectives

In this study, the wild-type and R484H mutant β-galactosidase enzymes from *B. circulans* ATCC 31382 were used to synthesize LGOS from lactulose. The optimal conditions for the production of LGOS were investigated in this study (Fig. 1). The wild-type enzyme had a highest yield of 202.9 ± 2.3 g/L (33.8% (w/w)) at 15 U/g lactulose, 60% (w/w) lactulose, and 60 °C incubated for 8 h. The R484H mutant enzyme had a highest yield of 197.7 ± 5.4 g/L (33.0% (w/w)) at 15 U/g lactulose, 60% (w/w) lactulose, 60 °C incubated for 16 h. When incubated with lactose, both enzymes reached a much higher GOS yield, i.e. 63.5% (w/w) for WT and 60.6% (w/w) for R484H [41], indicating that lactulose is not as good a substrate for this enzyme. Although the LGOS yields were lower than yields previously reported for *A. oryzae* (~50% (w/w)) and *K. marxianus* (~45% (w/w)) β-galactosidases [36,37], our data show a higher variety of LGOS structures.

Analysis by NMR spectroscopy and MALDI-TOF-MS identified 6 trisaccharides and 3 tetrasaccharides after separation with HPAEC-PAD, 6 of which (structures **1**, **2a**, **5**, **6**, **7a** and **7b**) had not been identified before. In previous studies, four LGOS structures were reported in total [16,34–37]. The LGOS product profiles of the wild-type BgaD-D and R484H mutant enzymes showed a difference in preference for introducing (β1→4) linkages and (β1→3) linkages. Our previous study showed that when lactose was used as substrate, the wild-type enzyme had a strong preference for (β1→4) linkages in GOS, only a trace amount of a (β1→3) linked trisaccharide was produced [41]. Here, however, when lactulose was used as substrate, the equivalent (β1→3) linked trisaccharide was the second largest peak in the LGOS profile of the wild-type enzyme (Fig. 3). Previously we have shown that mutant R484H also has a preference to introduce (β1→3) as well as (β1→4) linkages when incubated with lactose [41]. Here with lactulose as substrate a higher level of (β1→3)-linked structures was observed than for the WT enzyme, fitting with previous observations [41].

4. Materials and methods

4.1. Enzymes, chemicals, and strains

The wild-type BgaD-D and R484H mutant β-galactosidase enzymes of *B. circulans* ATCC 31382 are described in a previous study [41]. Lactulose (≥95%) was purchased from Sigma-Aldrich (Austria), galactose (≥99%), and acetonitrile was purchased from Boom (Meppel, Netherlands), fructose (≥99%) was purchased from Sigma (St Louis, USA).

4.2. Enzymatic synthesis of oligosaccharides from lactulose

For the production of LGOS, 10 U/mL of the wild-type BgaD-D and R484H mutant β-galactosidases (total enzyme activity towards lactose) were incubated with 50% (w/w) lactulose as substrate, at 50 °C for 20 h. The enzymes were inactivated by incubation at 100 °C for 10 min.

4.3. Optimization of LGOS yield

Several conditions were evaluated to optimize the production of LGOS with the wild-type and R484H mutant β-galactosidase enzymes of *B. circulans*. Firstly, enzyme amounts of 5 U/mL, 10 U/mL, 15 U/mL (total enzyme activity towards lactose) were incubated with a 50% (w/w) lactulose solution and incubated at 50 °C for 8 h for wild-type and

mutant enzymes. The reactions were stopped by heating at 100 °C for 10 min. Based on the obtained optimal enzyme amount, different lactulose concentrations (40%, 50%, 60% (w/w)) were also tested for both enzymes to obtain the optimal substrate concentration. Then, reaction temperatures (40 °C, 50 °C, 60 °C) were tested using the optimal enzyme amount and substrate concentration. In the last step, the reaction duration (8 h, 16 h, 24 h) was tested at the optimal conditions obtained above. All the samples were diluted 2000 times with Milli-Q water for HPAEC-PAD analysis. The quantification of LGOS yield was based on the calibration curve of galactose, fructose, and lactulose from 0.005 mM to 1.5 mM. LGOS yield = Initial lactulose – (remaining lactulose + galactose + fructose).

4.4. Separation of LGOS by Bio-Gel P2 column

The LGOS produced by the R484H mutant enzyme were diluted four times with Milli-Q water, and then loaded onto the Bio-Gel P2 column to separate the oligosaccharides. The LGOS were eluted with 10 mM ammonium carbonate. Samples of 3 mL were collected for each fraction and loaded on a High pH Anion Exchange Chromatography (HPAEC) coupled with an ICS3000 Pulsed Amperometric Detector (PAD). The fractions were separated on a CarboPac PA1 analytical column (2 × 250 mm) using a gradient described previously [42]. Fractions with similar profiles were pooled together (pool 1–4).

4.5. MALDI-TOF-MS analysis

The DP of the LGOS produced by the wild-type and R484H mutant enzymes was analyzed by MALDI-TOF-MS. The samples were mixed with 1 μL of 2,5-dihydroxybenzoic acid (10 mg/mL) in 40% (v/v) acetonitrile in a ratio of 1:1, and crystallized under atmospheric conditions. The experiments were carried out on an Axima performance mass spectrometer (Shimadzu Kratos Inc., Manchester, UK), equipped with a nitrogen laser (337 nm, 3 ns pulse width). Masses were calibrated using malto-oligosaccharides from DP2 to 8 as the external calibration ladder.

4.6. Isolation of LGOS fractions using HPAEC-PAD

The sample pools after the Bio-Gel P2 column were further separated by HPAEC-PAD using a CarboPac PA1 Semi-Preparative column (9 × 250 mm) on a Dionex ICS-5000 work station. The program used a complex gradient of A (100 mM NaOH), B (600 mM NaOAc in 100 mM NaOH), C (Milli-Q water), and D (50 mM NaOAc). The isolation was performed at 4.0 mL/min with 40% A, 0% B, 10% C, and 50% D to 50.3% A, 5.1% B, 7.4% C, and 37.2% D in 27 min. This was followed by washing with 100% B for 5 min and reconditioning with 40% A, 0% B, 10% C, and 50% D for 5 min. The collected fractions were neutralized with 4 M acetic acid immediately after the isolation. Desalting was performed on Extract Clean Carbo Columns (150 mg; Grace Davison Discovery Sciences).

4.7. NMR spectroscopy

Samples were exchanged twice with 300 μL D_2O (99.9 $_{atom}$%; Cambridge Isotope Ltd, Andover, MA), and finally dissolved in 650 μL D_2O containing internal acetone (δ_H 2.225 ppm, δ_C 31.08 ppm). One- and two-dimensional $^1H/^{13}C$ NMR spectra were recorded on a Varian Inova 500 MHz spectrometer (NMR department, University of Groningen) at a probe temperature of 25 °C. All spectra were recorded with a spectral width of 4000 Hz for ^1H, centered on the HOD signal and 15000 Hz for ^{13}C. One-dimensional ^1H NMR spectra were recorded, using a WET1D suppression pulse on the HOD signal, collecting 16–64 cumulative transients of 16 k complex data points. Two-dimensional NMR spectra (COSY, TOCSY 50 m s, 150 m s and ROESY) were recorded collecting 8–32 transients of 2000–4000 complex points per increment, collecting 200 increments. Gradient HSQC spectra with multiplicity editing were recorded collecting 32–64 cumulative transients of per increment, collecting 128–200 increments. All spectra were processed using MestReNova 9.1 (MestReLabs, Santiago de Compostella, Spain).

Acknowledgments

This work was financed by China Scholarship Council (to HY) and by the University of Groningen (to LD and SvL).

Appendix A. Supplementary data

Supplementary data related to this article can be found at http://dx.doi.org/10.1016/j.carres.2018.06.009.

References

[1] F. Zokaee, T. Kaghazchi, A. Zare, M. Soleimani, Isomerization of lactose to lactulose—study and comparison of three catalytic systems, Process Biochem. 37 (2002) 629–635.
[2] M. Aider, D. de Halleux, Isomerization of lactose and lactulose production: review, Trends Food Sci. Technol. 18 (2007) 356–364.
[3] A. Montilla, M.D. Del Castillo, M.L. Sanz, A. Olano, Egg shell as catalyst of lactose isomerisation to lactulose, Food Chem. 90 (2005) 883–890.
[4] Q. Shen, R. Yang, X. Hua, F. Ye, H. Wang, W. Zhao, K. Wang, Enzymatic synthesis and identification of oligosaccharides obtained by transgalactosylation of lactose in the presence of fructose using β-galactosidase from Kluyveromyces lactis, Food Chem. 135 (2012) 1547–1554.
[5] H. Wang, R. Yang, X. Hua, W. Zhao, W. Zhang, Enzymatic production of lactulose and 1-lactulose: Current state and perspectives, Appl. Microbiol. Biotechnol. 97 (2013) 6167–6180.
[6] M.R. Al Sibae, B.M. McGuire, Current trends in the treatment of hepatic encephalopathy, Therapeut. Clin. Risk Manag. 5 (2009) 617–626.
[7] C. Schumann, Medical, nutritional and technological properties of lactulose. An update, Eur. J. Nutr. 41 (2002) 17–25.
[8] H. Zhang, W. Chen, In vitro fermentation of lactulose by human gut bacteria, J. Agric. Food Chem. 62 (2014) 10970–10977.
[9] K.M. Tuohy, C.J. Ziemer, A. Klinder, Y. Knö Bel, B.L. Pool-Zobel, G.R. Gibson, A human volunteer study to determine the prebiotic effects of lactulose powder on human colonic microbiota, Ecol. Health Dis. 14 (2002) 165–173.
[10] J.P. Chae, E.A.B. Pajarillo, C.S. Park, D.K. Kang, Lactulose increases bacterial diversity and modulates the swine faecal microbiome as revealed by 454-pyrosequencing, Anim. Feed Sci. Technol. 209 (2015) 157–166.
[11] R. Palframan, G.R. Gibson, R.A. Rastall, Development of a quantitative tool for the comparison of the prebiotic effect of dietary oligosaccharides, Lett. Appl. Microbiol. 37 (2003) 281–284.
[12] K. Tuohy, G. Rouzaud, W. Bruck, G. Gibson, Modulation of the human gut microflora towards improved health using prebiotics - assessment of efficacy, Curr. Pharmaceut. Des. 11 (2005) 75–90.
[13] A. Olano, N. Corzo, Lactulose as a food ingredient, J. Sci. Food Agric. 89 (2009) 1987–1990.
[14] N. Seki, H. Saito, Lactose as a source for lactulose and other functional lactose derivatives, Int. Dairy J. 22 (2012) 110–115.
[15] A. Cardelle-Cobas, A. Olano, N. Corzo, M. Villamiel, M. Collins, S. Kolida, R.A. Rastall, In vitro fermentation of lactulose-derived oligosaccharides by mixed fecal microbiota, J. Agric. Food Chem. 60 (2012) 2024–2032.
[16] M. Corzo-Martínez, P. Copoví, A. Olano, F.J. Moreno, A. Montilla, Synthesis of prebiotic carbohydrates derived from cheese whey permeate by a combined process of isomerisation and transgalactosylation, J. Sci. Food Agric. 93 (2013) 1591–1597.
[17] C. Guerrero, C. Vera, F. Plou, A. Illanes, Influence of reaction conditions on the selectivity of the synthesis of lactulose with microbial β-galactosidases, J. Mol. Catal. B Enzym. 72 (2011) 206–212.
[18] N.M. Delzenne, Oligosaccharides: state of the art, Proc. Nutr. Soc. 62 (2003) 177–182.
[19] G. Dongowski, G. Jacobasch, D. Schmiedl, Structural stability and prebiotic properties of resistant starch type 3 increase bile acid turnover and lower secondary bile acid formation, J. Agric. Food Chem. 53 (2005) 9257–9267.
[20] O. Hernández-Hernández, A. Muthaiyan, F.J. Moreno, A. Montilla, M.L. Sanz, S.C. Ricke, Effect of prebiotic carbohydrates on the growth and tolerance of Lactobacillus, Food Microbiol. 30 (2012) 355–361.
[21] R.A. Rastall, G.R. Gibson, H.S. Gill, F. Guarner, T.R. Klaenhammer, B. Pot, G. Reid, I.R. Rowland, M.E. Sanders, Modulation of the microbial ecology of the human colon by probiotics, prebiotics and synbiotics to enhance human health: an overview of enabling science and potential applications, FEMS Microbiol. Ecol. 52 (2005) 145–152.
[22] A. Cardelle-Cobas, N. Corzo, A. Olano, C. Peláez, T. Requena, M. Ávila, Galactooligosaccharides derived from lactose and lactulose: influence of structure on Lactobacillus, Streptococcus and Bifidobacterium growth, Int. J. Food Microbiol. 149 (2011) 81–87.
[23] A. Cardelle-Cobas, M. Fernández, N. Salazar, C. Martínez-Villaluenga, M. Villamiel,

P. Ruas-Madiedo, C.G. de los Reyes-Gavilán, Bifidogenic effect and stimulation of short chain fatty acid production in human faecal slurry cultures by oligosaccharides derived from lactose and lactulose, J. Dairy Res. 76 (2009) 317–325.
[24] O. Hernández-Hernández, M.C. Marín-Manzano, L.A. Rubio, F.J. Moreno, M.L. Sanz, A. Clemente, Monomer and linkage type of galacto-oligosaccharides affect their resistance to ileal digestion and prebiotic properties in rats, J. Nutr. 142 (2012) 1232–1239.
[25] F. Algieri, A. Rodríguez-Nogales, N. Garrido-Mesa, T. Vezza, J. Garrido-Mesa, M.P. Utrilla, A. Montilla, A. Cardelle-Cobas, A. Olano, N. Corzo, E. Guerra-Harnández, A. Zarzuelo, M.E. Rodriguez-Cabezas, J. Galvez, Intestinal anti-inflammatory effects of oligosaccharides derived from lactulose in the trinitrobenzenesulfonic acid model of rat colitis, J. Agric. Food Chem. 62 (2014) 4285–4297.
[26] D.L. Topping, P.M. Clifton, Short-chain fatty acids and human colonic function: roles of resistant starch and nonstarch polysaccharides, Physiol. Rev. 81 (2001) 1031–1064.
[27] S. Macfarlane, G.T. Macfarlane, J.H. Cummings, Review article: prebiotics in the gastrointestinal tract, Aliment. Pharmacol. Ther. 24 (2006) 701–714.
[28] M.C. Marín-Manzano, L. Abecia, O. Hernández-Hernández, M.L. Sanz, A. Montilla, A. Olano, L.A. Rubio, F.J. Moreno, A. Clemente, Galacto-oligosaccharides derived from lactulose exert a selective stimulation on the growth of Bifidobacterium animalis in the large intestine of growing rats, J. Agric. Food Chem. 61 (2013) 7560–7567.
[29] J.M. Laparra, O. Hernandez-Hernandez, F.J. Moreno, Y. Sanz, Neoglycoconjugates of caseinomacropeptide and galactooligosaccharides modify adhesion of intestinal pathogens and inflammatory response(s) of intestinal (Caco-2) cells, Food Res. Int. 54 (2013) 1096–1102.
[30] J.M. Laparra, M. Díez-Municio, M. Herrero, F.J. Moreno, Structural differences of prebiotic oligosaccharides influence their capability to enhance iron absorption in deficient rats, Food Funct. 5 (2014) 2430–2437.
[31] S.S. van Leeuwen, B.J.H. Kuipers, L. Dijkhuizen, J.P. Kamerling, 1H NMR analysis of the lactose/β-galactosidase-derived galacto-oligosaccharide components of Vivinal® GOS up to DP5, Carbohydr. Res. 400 (2014) 59–73.
[32] S.S. van Leeuwen, B.J.H. Kuipers, L. Dijkhuizen, J.P. Kamerling, Corrigendum to “1H NMR analysis of the lactose/β-galactosidase-derived galacto-oligosaccharide components of Vivinal® GOS up to DP5”, Carbohydr. Res. 400 (2014) (2016) 59–73 Carbohydr. Res. 419:69-70.
[33] S.S. van Leeuwen, B.J.H. Kuipers, L. Dijkhuizen, J.P. Kamerling, Comparative structural characterization of 7 commercial galacto-oligosaccharide (GOS) products, Carbohydr. Res. 425 (2016) 48–58.
[34] A. Cardelle-Cobas, C. Martínez-Villaluenga, M. Villamiel, A. Olano, N. Corzo, Synthesis of oligosaccharides derived from lactulose and Pectinex Ultra SP-L, J. Agric. Food Chem. 56 (2008) 3328–3333.
[35] A. Cardelle-Cobas, N. Corzo, C. Martínez-Villaluenga, A. Olano, M. Villamiel, Effect of reaction conditions on lactulose-derived trisaccharides obtained by transgalactosylation with β-galactosidase of Kluyveromyces lactis, Eur. Food Res. Technol. 233 (2011) 89–94.
[36] B. Padilla, A.I. Ruiz-Matute, C. Belloch, A. Cardelle-Cobas, N. Corzo, P. Manzanares, Evaluation of oligosaccharide synthesis from lactose and lactulose using β-galactosidases from Kluyveromyces isolated from artisanal cheeses, J. Agric. Food Chem. 60 (2012) 5134–5141.
[37] A. Cardelle-Cobas, A. Olano, G. Irazoqui, C. Giacomini, F. Batista-Viera, N. Corzo, M. Corzo-Martínez, Synthesis of oligosaccharides derived from lactulose (LGOS) using soluble and immobilized Aspergillus oryzae β-galactosidase, Front. Bioeng. Biotechnol 4 (2016) 21.
[38] O. Hernández-Hernández, F. Montañés, A. Clemente, F.J. Moreno, M.L. Sanz, Characterization of galactooligosaccharides derived from lactulose, J. Chromatogr. a 1218 (2011) 7691–7696.
[39] J. Song, H. Imanaka, K. Imamura, M. Minoda, T. Katase, Y. Hoshi, S. Yamaguchi, K. Nakanishi, Cloning and expression of a β-galactosidase gene of Bacillus circulans, Biosci. Biotechnol. Biochem. 75 (2011) 1194–1197.
[40] K. Ishikawa, M. Kataoka, T. Yanamoto, M. Nakabayashi, M. Watanabe, S. Ishihara, S. Yamaguchi, Crystal structure of β-galactosidase from Bacillus circulans ATCC 31382 (BgaD) and the construction of the thermophilic mutants, FEBS J. 282 (2015) 2540–2552.
[41] H. Yin, T. Pijning, X. Meng, L. Dijkhuizen, S.S. van Leeuwen, Engineering of the Bacillus circulans β-galactosidase product specificity, Biochemistry 56 (2017) 704–711.
[42] H. Yin, J.B. Bultema, L. Dijkhuizen, S.S. van Leeuwen, Reaction kinetics and galactooligosaccharide product profiles of the β-galactosidases from Bacillus circulans, Kluyveromyces lactis and Aspergillus oryzae, Food Chem. 225 (2017) 230–238.
[43] J. Mayer, J. Conrad, I. Klaiber, S. Lutz-Wahl, U. Beifuss, L. Fischer, Enzymatic production and complete nuclear magnetic resonance assignment of the sugar lactulose, J. Agric. Food Chem. 52 (2004) 6983–6990.
[44] A. Cardelle-Cobas, N. Corzo, M. Villamiel, A. Olano, Isomerization of lactose-derived oligosaccharides: a case study using sodium aluminate, J. Agric. Food Chem. 56 (2008) 10954–10959.